Mi *et al.*
Low-carbon Materials and Green Construction (2023) 1:21
https://doi.org/10.1007/s44242-023-00024-4

Low-carbon Materials
and Green Construction

ORIGINAL ARTICLE

Open Access

Effects of carbon-sequestering coral aggregate on pore structures and compressive strength of concrete

Renjie Mi[1*†], Yifei Wang[1†], Tao Yu[1] and Wengui Li[2]

Abstract

CO_2 sequestration/storage shows considerable impacts on the pore structures and compressive strength of concrete. This paper presents a study in which coral aggregates were presoaked in $Ca(OH)_2$ slurries with different solid-to-liquid ratios (i.e. 0.2, 0.4, and 0.6 g/mL) followed by accelerated carbonation. The effects of CO_2 sequestration on the particle size distribution, cylinder compressive strength, water absorption, and apparent density of coral aggregate were investigated. The evolution of pore structures in coral aggregate concrete after CO_2 sequestration was also studied. Additionally, the effect of CO_2 sequestration on the development of compressive strength of coral aggregate concrete was explored. The results showed that CO_2 sequestration affected the properties of coral aggregate. Moreover, the porosity of $CaCO_3$ formed by CO_2 sequestration was the highest in the concrete. With the increase of solid-to-liquid ratio, the porosity of cement pastes and the $CaCO_3$ increased, and more big pores existed in the cement pastes and $CaCO_3$. Furthermore, the compressive strength of coral aggregate concrete when the solid-to-liquid ratio was 0.2 g/mL increased compared with that before CO_2 sequestration, but the compressive strength reduced when the ratio increased to 0.6 g/mL.

Keywords CO_2 sequestration, Coral aggregate concrete, Compressive strength, Pore structures

摘 要

二氧化碳封存对混凝土的孔结构和抗压强度有较大影响。本文首先将珊瑚骨料分别浸泡在固液比为0.2、0.4和0.6 g/mL的氢氧化钙悬浮液中，然后将浸泡后的骨料加速碳化。其次，研究了二氧化碳封存对珊瑚骨料的粒径分布、筒压强度、吸水率和表观密度的影响。再次，研究了二氧化碳封存后珊瑚骨料混凝土的孔结构演变。最后，探讨了二氧化碳封存对珊瑚骨料混凝土抗压强度发展的影响。结果表明，二氧化碳封存影响了珊瑚骨料的性能。其次，在混凝土中，通过二氧化碳封存形成的碳酸钙的孔隙率最高。随着固液比的增大，水泥基体和该碳酸钙的孔隙率逐渐增大，且水泥基体和该碳酸钙中存在更多的大孔。最后，当固液比为0.2 g/mL时，珊瑚骨料混凝土的抗压强度较二氧化碳封存前有所提高，但当固液比增加到0.6 g/mL时，其抗压强度有所降低。

关键词 二氧化碳封存, 珊瑚骨料混凝土, 抗压强度, 孔结构

†Renjie Mi and Yifei Wang contributed equally to this work.

*Correspondence:
Renjie Mi
renjiemi3-c@my.cityu.edu.hk
Full list of author information is available at the end of the article

1 Introduction

Mineral carbonation is regarded as a promising technology to capture and utilise anthropogenic CO_2 [1]. Cement-based materials, the second most consumed materials after water on earth [2], provide considerable space for mineral carbonation. Specifically, CO_2 can be sequestered by industrial by-products [3], recycled aggregates [4], and the hardened cement pastes of concrete [5]. However, when CO_2 is sequestered in the cement pastes, the pH value of concrete pore solution reduces [6], and the steel reinforcement in the concrete may corrode.

To avoid such weakness, Mi et al. [7] proposed a new CO_2 sequestering method by utilising the open pores of porous aggregates (e.g., coral aggregates, waste clay brick aggregates, lightweight aggregates, etc.); this method includes two stages: (1) presoaking the aggregates in an alkaline slurry, and (2) curing the presoaked aggregates in a carbonation tank. As expected, the results of Mi et al. [7] showed that the pH value of concrete pore solution was not affected using such new method. Additionally, the study [7] showed that the development of compressive strength of coral aggregate concrete (CAC) was little affected when the solid-to-liquid (S/L) ratio of the slurry was 0.4 g/mL. However, the effect of this method on the development of compressive strength under a wider S/L ratio has not been systematically explored in the study [7].

The development of compressive strength of CAC without CO_2 sequestration has been investigated in many studies. For example, the results of Da et al. [8] revealed that although the compressive strength of normal concrete was higher than that of CAC because coral aggregate was more fragile than natural aggregate, a stronger interfacial transition zone (ITZ) formed due to the rough surface and internal curing regime of coral aggregate [9]. Wu et al. [10] further explored the compressive strength of CAC with fly ash and silica fume and the results showed that the combination of such by-products promoted the long-term compressive strength of CAC. Additionally, Wang et al. [11] modified the coral aggregate by a superfine cement paste; but the compressive strength of the corresponding concrete was lower than that of normal concrete. Chu et al. [12] further modified coral aggregates using basic magnesium sulfate cement; the compressive strength of concrete with such modified aggregates was improved by 31.8% compared with normal CAC. Similarly, Liu et al. [13] presoaked coral aggregates using sodium silicate and granulated blast furnace slag; as expected, the compressive strength of relevant concrete was 26.9% greater than that of the untreated CAC.

To better understand and improve the compressive strength of concrete, its pore structures were investigated using various techniques [14]. For example, Chen et al. [15] studied the porosity (pore size: larger than 100 nm) of ITZ in concrete based on a two-dimensional image obtained using a backscattered electron image analysis approach. For CAC, the evolution of pore characteristics of ITZ between cement pastes and coral aggregates presoaked by supplementary cementitious materials was investigated using the Scanning Electron Microscope (SEM) approach [12, 13]. Although the above two-dimensional techniques provided great research progress, the results cannot reflect the actual microstructure in three-dimensions. Therefore, Chung et al. [16] investigated the actual pore structures of ITZ in three-dimensions using the microcomputed tomography (micro-CT) technology.

Against above background, coral aggregate can be used to sequester/store CO_2, but the CO_2 sequestration might affect the development of compressive strength of CAC. In the authors' previous study, the properties of coral aggregate (Particle size: 5–20 mm) and relevant concrete were already investigated for a particular S/L ratio (i.e. 0.4 g/mL); but the effects of a wider S/L ratio on the properties were not studied [7]. Therefore, this study further explores the properties of coral aggregate (Particle size: 5–14 mm) after CO_2 sequestration using different S/L ratios (i.e. 0.2, 0.4 and 0.6 g/mL), and the resulting pore structures and compressive strength of CAC. The aims of this study are:

(1) to study the effects of CO_2 sequestration with different S/L ratios on the properties of coral aggregate;
(2) to investigate the evolution of pore structures in CAC after CO_2 sequestration; and
(3) to explore the effects of CO_2 sequestration with different S/L ratios on the development of compressive strength of CAC.

This study provides a better understanding for the development of compressive strength of CAC after CO_2 sequestration with different S/L ratios. This can help the engineers or academics design low-carbon CAC considering its CO_2 sequestration capability and compressive strength.

2 Materials and experiments

2.1 Materials

Coral reefs sourced from South China Sea were crushed as coarse coral aggregate (CCA) with a size of 5–14 mm in a jaw crusher. River sand was used as the fine aggregate and its fineness modulus was 2.6. The 52.5 CEM1 Portland cement used in this study was provided by Green Island Cement, Hong Kong. The properties and chemical composition of the cement are summarised in Tables 1 and 2, respectively. The tap water and a water reducer

Table 1 Properties of the cement

Specific surface area (m^2/kg)	Setting time (min)		Compressive strength (MPa)	
	Initial	Final	2 d	28 d
366	105	135	23.8	60.2

Table 2 Chemical composition of the cement (wt.%)

SiO_2	Al_2O_3	Fe_2O_3	CaO	MgO	Others
20.5	6.6	3.3	66.4	0.7	2.5

sourced from GCP Applied Technologies were used during the concrete preparation. The $Ca(OH)_2$ analytical reagent (Purity: > 95%) and CO_2 gas (Purity: > 99.8%) were provided by Tianjin Dengfeng Chemical Reagent Factory, China, and Linde HKO Limited, Hong Kong, respectively.

2.2 Experiments

2.2.1 Preparation of the specimens

Three kinds of $Ca(OH)_2$ slurries were prepared by mixing the $Ca(OH)_2$ analytical reagent with tap water with different S/L ratios (i.e. 0.2, 0.4, and 0.6 g/mL, respectively). CCAs were then completely soaked in a given $Ca(OH)_2$ slurry followed by a stir for 10 min. Subsequently, such aggregates were placed in a 50 ℃ oven and dried for 5 h. After that, the dried aggregates were placed in a carbonation chamber where the CO_2 concentration, temperature, and humidity were 20%, 20 ℃, and 70%, respectively. During the carbonation, the aggregates were stirred after every 24 h to ensure the complete reaction of the $Ca(OH)_2$ slurries in the pores with CO_2. To examine the carbonation degree of the $Ca(OH)_2$ powder in the aggregates, a 1% phenolphthalein alcohol solution was sprayed on the powder after every 24 h. The powder was considered fully carbonated if it did not discolour. The CCAs pre-soaked in above three kinds of slurries (i.e. 0.2, 0.4, and 0.6 g/mL) after carbonation were marked as CCA-0.2, CCA-0.4, and CCA-0.6, respectively; the CCA without the treatment was marked as CCA-0.

Four kinds of concrete specimens were prepared using CCA-0, CCA-0.2, CCA-0.4, and CCA-0.6 and the samples were marked as C-0, C-0.2, C-0.4, and C-0.6, respectively. The mix proportions of the concretes designed according to the Chinese standard T/CECS 694–2020 [17] and the Ref. [8] were given in Table 3. The coral aggregates (i.e. CCA-0, CCA-0.2, CCA-0.4, and CCA-0.6) were first saturated before concrete preparation based on the requirements of the Chinese standard T/CECS 694–2020 [17]. Water, the water reducer, and cement were then mixed in a mechanical mixer for 1 min at a speed of 122 rpm. Subsequently, the coral aggregate and river sand were added into the mixture and mixed for 1 min at the same speed. The mixture was mixed for another 1 min at a higher speed of 219 rpm.

2.2.2 Testing methods

2.2.2.1 Properties of the coral aggregates The physical properties (i.e. particle size distribution, apparent density, and water absorption) of the aggregates were tested based on the standard GB/T 50081–2019 [18], while the cylinder compressive strength of the aggregates was determined according to the standard GB/T 17431.2–2010 [19].

2.2.2.2 Slump and compressive strength of the concretes The slump of the fresh concrete specimens was determined according to the standard GB/T 50081–2019 [18]; the results are encapsuled in Table 3. Additionally, concrete specimens with the size of $100\times100\times100$ mm^3 were prepared and cured in a laboratory where the humidity was 99% and the temperature was 25°C. After being cured for different periods (i.e. 3, 7, 14, and 28 days, respectively), the compressive strength of the samples was tested in a MTS testing equipment with the loading rate of 0.5 MPa/s based on the standard GB/T 50081–2019 [18]. The compressive strength of each mixture was determined by three measurements.

2.2.2.3 Pore structures of the concretes X-ray images of the concrete specimens were obtained using a vivo microCT scanner (Bruker SkyScan 1276) with an applied Al-Cu filter. The X-ray source voltage, current, voxel

Table 3 Mix proportions of the concrete samples

Type	Effective w/c ratio	Water (kg/m^3)	Cement (kg/m^3)	Fine aggregate (kg/m^3)	Coarse aggregate		Water reducer (kg/m^3)	Slump (mm)
					Type	Weight (kg/m^3)		
C-0	0.3	150	500	873	CCA-0	582	4.5	121
C-0.2	0.3	150	500	873	CCA-0.2	582	4.7	123
C-0.4	0.3	150	500	873	CCA-0.4	582	4.9	126
C-0.6	0.3	150	500	873	CCA-0.6	582	5.1	130

size, and exposure time were set to be 90 kV, 200 μ A, 10.204 mμ, and 980 ms, respectively. A rotational step of 0.2 degree was applied to every projection. Subsequently, the associated software, NRecon (Skyscan, Kontich, Belgium), was used to reconstruct the obtained consistent volume of interest (VOI) for each specimen. The following optimal settings were set: (a) smoothing of 6, (b) ring artefact reduction of 12, and (c) beam hardening correction of 33%.

The VOIs generated by NRecon were further processed with CTAn (Skyscan, Kontich, Belgium) to conduct 3D analysis based on thresholding. Every pixel in a microCT image was represented by an 8-bit integer ranging from 0 to 255; the darkness of the corresponding pixel decreased with the number. All morphometric characteristics can only be analysed on the basis of binarised images, which were obtained via thresholding. Based on the Otsu method [20] and manual selection, 65, 100, and 155 were determined to be the threshold values distinguishing the pores and $CaCO_3$ formed by CO_2 sequestration, the cement pastes and $CaCO_3$ formed by CO_2 sequestration, and the cement pastes and original $CaCO_3$ in coral aggregate, respectively. One coral aggregate particle was selected for each specimen. To investigate the volume and distribution of pores, $CaCO_3$ formed by CO_2 sequestration and original $CaCO_3$ in coral aggregate within the selected aggregate particle, a region of interest (ROI) was drawn manually to isolate the aggregate particle from the surrounding materials.

After applying the corresponding threshold, 3D analysis was performed to obtain quantitative data on the porosity and pore size distribution for each object (i.e. pores, $CaCO_3$ formed by CO_2 sequestration, cement pastes, and original $CaCO_3$ in coral aggregate). A visual reconstruction of the contents within the ROI was created using CTvox (Skyscan, Kontich, Belgium). Moreover, the pore structures of original $CaCO_3$ in coral aggregate, cement pastes, and $CaCO_3$ formed by CO_2 sequestration were examined through selecting three ROIs for each of them in every specimen. With the 3D analysis results, the porosity of each type of materials was compared and the effects of slurries with different S/L ratios on the pore distribution in cement pastes were investigated. The result of porosity was determined by three measurements.

3 Results and discussion

3.1 Properties of the coral aggregates

The appearances of the coral aggregates are shown in Fig. 1. It is clear that CCA-0 was a porous aggregate with a lot of open pores (Fig. 1a), which can be used to sequester/store CO_2, as demonstrated in the authors' previous study [7]. According to the study [7], the powder in the pores of the aggregates was verified as $CaCO_3$. In this study, it is evident that some pores in CCA-0.2 were filled with $CaCO_3$ formed by CO_2 sequestration (Fig. 1b). With the increase of S/L ratio of the slurry, the open pores in the aggregates (i.e. CCA-0.4, and CCA-0.6) were filled with more $CaCO_3$ formed by CO_2 sequestration (Fig. 1c and d). Additionally, a clear $CaCO_3$ layer that formed by CO_2 sequestration was attached on the original coral aggregate in CCA-0.6 when the ratio increased to 0.6 g/mL (Fig. 1d).

The physical properties of the aggregates are presented in Fig. 2. It is evident that the difference of the cylinder compressive strength between CCA-0.2 and CCA-0 was very small (i.e. around 1.2%), as shown in Fig. 2a; but the strength of CCA-0.4 was slightly higher than that of CCA-0 by 7% (Fig. 2a) because more pores in CCA-0.4 were filled with $CaCO_3$ formed by CO_2 sequestration (Fig. 1c). This result is in good consistence with the study [7]. Interestingly, the strength of CCA-0.6 was smaller than that of CCA-0 by about 10% because a $CaCO_3$ layer attached on the original coral aggregate (Fig. 1d), and the layer may be a loose structure that contained a lot of pores, which has been verified in Sect. 3.2.2.

Additionally, the particle size distribution of the aggregates (i.e. CCA-0, CCA-0.2, and CCA-0.4) was slightly affected when the S/L ratio was smaller than 0.4 g/

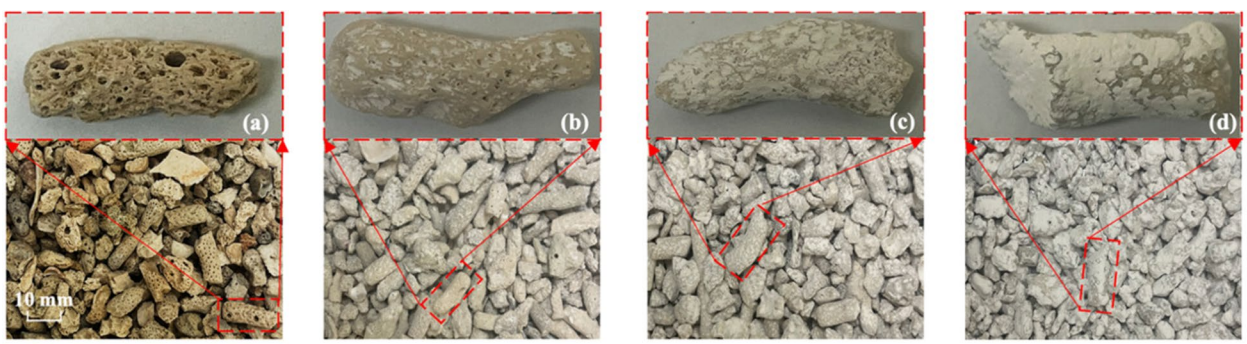

Fig. 1 Appearances of the CCAs: (**a**) CCA-0, (**b**) CCA-0.2, (**c**) CCA-0.4, and (**d**) CCA-0.6

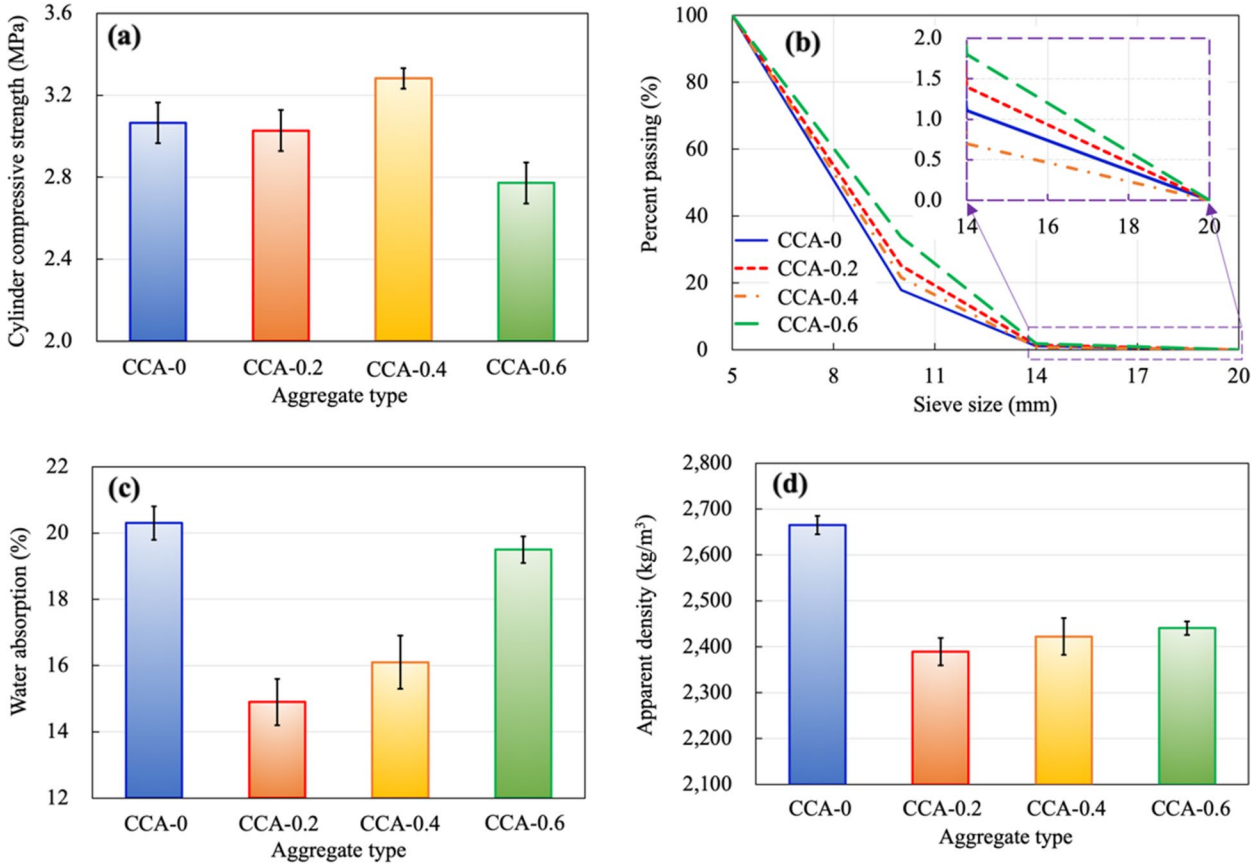

Fig. 2 Physical properties of the coral aggregates: (**a**) cylinder compressive strength, (**b**) particle size distribution, (**c**) water absorption, and (**d**) apparent density

mL (Fig. 2b). A clear difference, however, was observed for CCA-0.6 (S/L ratio: 0.6 g/mL). This is because the amount of larger aggregate increased as a $CaCO_3$ layer formed on the original aggregate surface (Fig. 1d) which increased the particle size.

Moreover, it is clear that the water absorption of the coral aggregate reduced by 5.4%-0.8% after CO_2 sequestration (Fig. 2c), which is consistent with the previous study [7]; the reduction decreased with the increase of S/L ratio. This is because the water absorption increases with the increase of amount of capillary pores [21]. With the increase of S/L ratio, the amount of macro pores in CCA filled by the $CaCO_3$ formed by CO_2 sequestration increased (Fig. 1) and the capillary pores in the $CaCO_3$ increased as well. A similar law can also be deduced for the apparent density (Fig. 2d). Due to the formation of the $CaCO_3$, the density of CCA reduced by 10.3%-8.4%; with the increase of S/L ratio, the reduction decreased. The decrease of apparent density might be explained by the fact that the increase of volume of the aggregate was greater than the increase of mass of the aggregate because the $CaCO_3$ closed some open pores but did not fully fill them.

3.2 Pore structures of the concretes

3.2.1 Pore distributions

Figure 3 summarises the representative images for the pore distributions in the concretes before and after CO_2 sequestration. Clearly, a lot of big open pores still existed in C-0 (Fig. 3a). Therefore, the pores can be used to sequester/store CO_2. Some pores in C-0.2 were filled with the $CaCO_3$ formed by CO_2 sequestration, while the others were still empty (Fig. 3b). With the increase of S/L ratio, more pores in the coral aggregates (i.e. CCA-0.4 and CCA-0.6) were filled with the $CaCO_3$ (Fig. 3c and d). Interestingly, some big pores existed in the $CaCO_3$ formed by CO_2 sequestration (Fig. 3d), which means that the slurry normally attached on the inner surface of the aggregates. Therefore, a lot of spaces still existed in the coral aggregates (i.e. CCA-0.6) even though the S/L ratio of the slurry was 0.6 g/mL.

Additionally, some big pores existed near the coral aggregates (Figs. 3c and d); these pores can be regarded

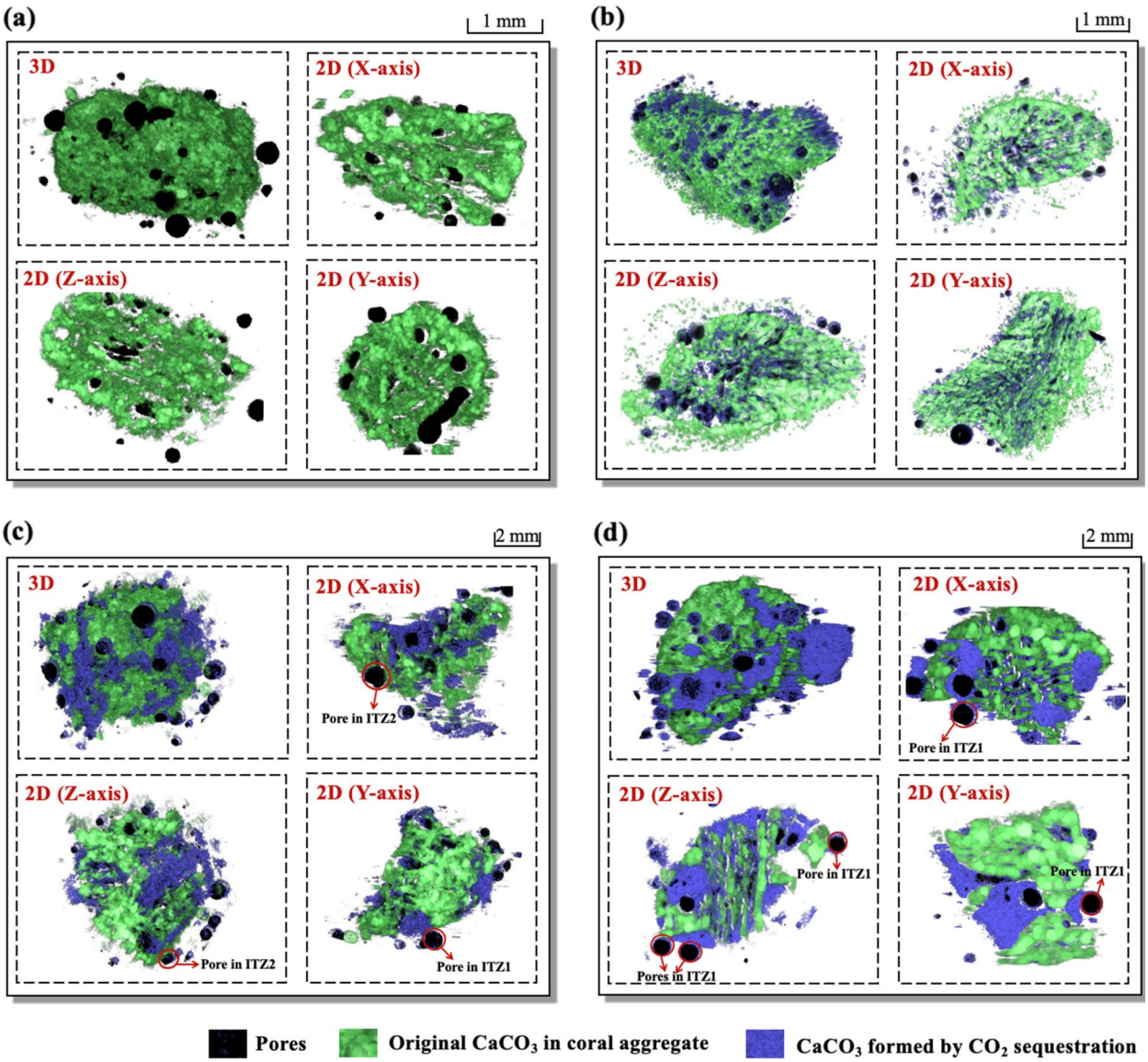

Fig. 3 Pore distributions in the concretes: (**a**) C-0, (**b**) C-0.2, (**c**) C-0.4, and (**d**) C-0.6. Notes. ITZ1 refers to the ITZ between $CaCO_3$ formed by CO_2 sequestration and cement pastes; ITZ2 refers to the ITZ between original $CaCO_3$ in coral aggregate and cement pastes

as the pores in the ITZs and may affect the properties of the concrete [22, 23]. Owing to the addition of $CaCO_3$, three kinds of ITZs (i.e. between $CaCO_3$ formed by CO_2 sequestration and original $CaCO_3$ in coral aggregate, between $CaCO_3$ formed by CO_2 sequestration and cement pastes, and between cement pastes and original $CaCO_3$ in coral aggregate) existed in CAC. It is evident that some big pores existed in the ITZ between $CaCO_3$ formed by CO_2 sequestration and cement pastes (Fig. 3c and d), and the ITZ between original $CaCO_3$ in coral aggregate and cement pastes (Fig. 3c), whereas no big pore was observed in the ITZ between $CaCO_3$ formed by CO_2 sequestration and original $CaCO_3$ in coral aggregate. This is because the absorbed water in original coral aggregate and $CaCO_3$ formed by CO_2 sequestration before mixing gradually flowed into cement pastes during the internal curing. Therefore, the water/cement ratio of the ITZs was higher than that of cement pastes; more pores existed in the ITZs compared with cement pastes.

3.2.2 Porosity

The porosity of cement pastes, $CaCO_3$ formed by CO_2 sequestration, and original $CaCO_3$ in coral aggregate is depicted in Fig. 4. It is clear that the porosity of $CaCO_3$ formed by CO_2 sequestration was much higher than that of cement pastes; the figure of cement pastes was much

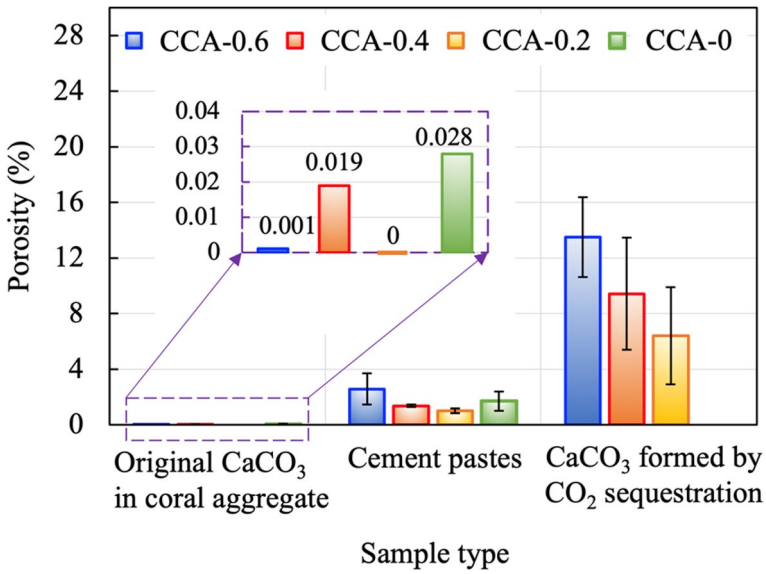

Fig. 4 Porosity of cement pastes, $CaCO_3$ formed by CO_2 sequestration, and original $CaCO_3$ in coral aggregate

greater than that of original $CaCO_3$ in coral aggregate. Therefore, $CaCO_3$ formed by CO_2 sequestration was the most porous structure in the concrete, which demonstrated the results of cylinder compressive strength of CCA-0.6 (Fig. 2a). Additionally, with the increase of S/L ratio from 0.2–0.6 g/mL, the porosity of cement pastes increased. This is because the porosity of $CaCO_3$ formed by CO_2 sequestration increased with the increase of S/L ratio. Therefore, more water released from the $CaCO_3$ and increased the effective water/cement ratio of cement pastes.

3.2.3 Pore size distributions

The pore size distributions of cement pastes and $CaCO_3$ formed by CO_2 sequestration in the concretes are shown in Fig. 5. It is clear that with the increase of S/L ratio, more big pores with the size of over 326 μm existed in the cement pastes (Fig. 5a), whereas the proportion of pores smaller than 326 μm reduced. Additionally, with the increase of S/L ratio, more big pores with the size of over 60 μm existed in the $CaCO_3$, whereas the proportion of pores smaller than 60 μm reduced. The increase of proportion of big pores in cement pastes and the $CaCO_3$ may show negative effects on the compressive strength of concrete because the strength was affected by big pores [24].

3.3 Development of compressive strength of the concretes

The development of compressive strength of the concretes is shown in Fig. 6. The strengths of coral aggregate, cement pastes, and their ITZ are the major contributors to the compressive strength of the concrete. It is revealed that the ITZ was the strongest part in CAC as the damages were observed in the coral

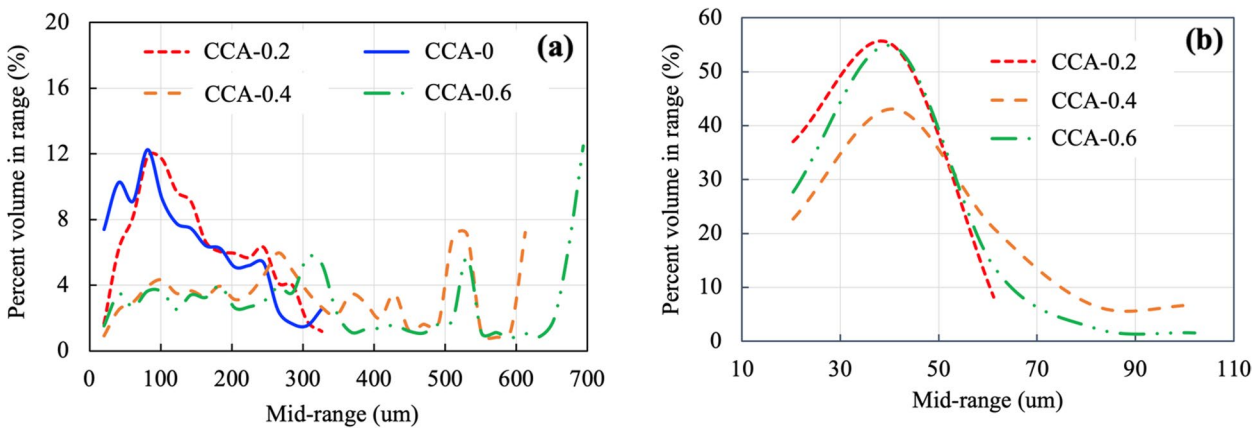

Fig. 5 Pore size distributions of (**a**) cement pastes, and (**b**) $CaCO_3$ formed by CO_2 sequestration

aggregate and cement pastes, which can be ascribed to the rough surface and internal curing regime of coral aggregate [8]. In this study, it is evident that the compressive strengths of C-0.2 after curing 3–28 d were greater than those of C-0 by 9.9–16%. This is because the water absorption of CCA-0.2 was smaller than that of CCA-0 by 3.2% (Fig. 2c). The amount of absorbed water in CCA-0.2 that flowed into the cement pastes and ITZ and further participated the hydration in CCA-0.2 reduced.

Interestingly, the differences of compressive strengths between C-0.4 and C-0 were within 1%, indicating that the strength development of concrete was not affected if the S/L ratio was 0.4 g/mL. This is in consistent with the authors' previous study [7]. Although the cylinder compressive strength of CCA-0.4 was greater than that of CCA-0 (Fig. 2a), the strengths of hardened cement pastes and $CaCO_3$ formed by CO_2 sequestration in C-0.4 reduced because the proportion of big pores in the cement pastes and $CaCO_3$ increased (Fig. 5). Additionally, the strength of ITZs in C-0.4 reduced. The pores in CCA-0.4 were filled with $CaCO_3$ (Fig. 3c), and two kinds of new ITZs (i.e. between $CaCO_3$ formed by CO_2 sequestration and original $CaCO_3$ in coral aggregate, and between $CaCO_3$ formed by CO_2 sequestration and cement pastes) formed in C-0.4. As the density of $CaCO_3$ formed by CO_2 sequestration was much lower than that of original $CaCO_3$ in coral aggregate because the porosity of the former was much higher than that of the latter (Fig. 4), the new ITZs were weaker than the old ITZ between cement pastes and original aggregate. The reduction of strength of ITZ in C-0.4 was offset by the increase of cylinder compressive strength of CCA-0.4.

For C-0.6, its compressive strengths after curing 3–28 d were smaller than those of C-0 by 0.3–13.3%, which means that increasing the S/L ratio to 0.6 g/mL may reduce the compressive strength of concrete. This can be mainly attributed to the reduction of cylinder compressive strength of CCA-0.6 (Fig. 2a) and the increase of number of big pores of hardened cement pastes (Fig. 5a) and $CaCO_3$ formed by CO_2 sequestration (Fig. 5b). Besides, the original aggregate was covered by $CaCO_3$ (Fig. 1d). Therefore, two kinds of new ITZs (i.e. between $CaCO_3$ formed by CO_2 sequestration and original $CaCO_3$ in coral aggregate, and between $CaCO_3$ formed by CO_2 sequestration and cement pastes) formed. The overall strength of these two kinds of ITZs was lower than that of original ITZ between coral aggregate and cement pastes in C-0 because the porosity of the $CaCO_3$ formed by CO_2 sequestration was much higher than that of the original $CaCO_3$ in coral aggregate (Fig. 4).

4 Conclusions

This paper has investigated the properties of coral aggregate after CO_2 sequestration using different S/L ratios (0.2, 0.4 and 0.6 g/mL), and the pore structures and compressive strength of CAC. The main conclusions are as follows:

(1) The effects of the slurry with a S/L ratio of 0.2 g/mL on the particle size distribution and cylinder compressive strength of CCA were very slight. The strength of CCA increased when the S/L ratio increased to 0.4 g/mL. If the ratio increased to 0.6 g/mL, the strength of CCA reduced, but its particle

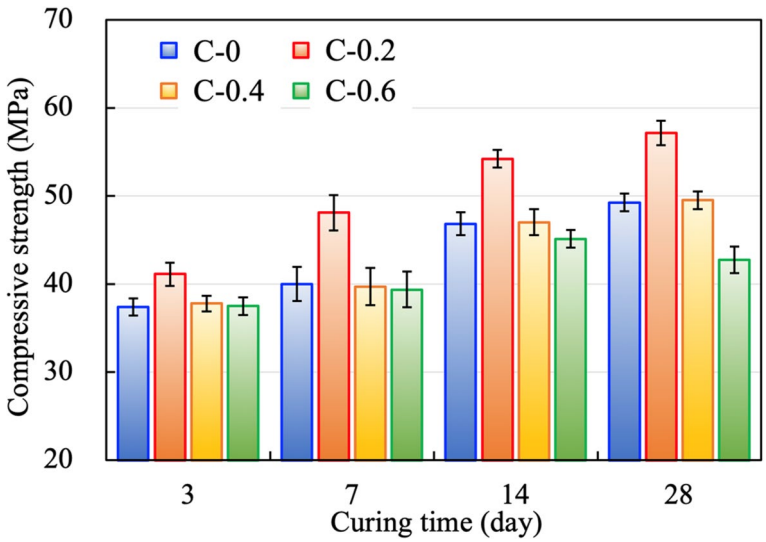

Fig. 6 Development of compressive strength of the coral aggregate concretes at different curing ages

size increased. Moreover, the water absorption and apparent density of CCA after CO_2 sequestration reduced; increasing the S/L ratio can increase the water absorption and apparent density.
(2) After CO_2 sequestration, some big pores still existed in the $CaCO_3$ formed by CO_2 sequestration and near the coral aggregates. Additionally, the porosity of $CaCO_3$ formed by CO_2 sequestration was the highest in the concrete. With the increase of S/L ratio, the porosity of cement pastes and the $CaCO_3$ increased, and more big pores existed in the cement pastes and $CaCO_3$ formed by CO_2 sequestration.
(3) The compressive strengths of CAC when the S/L ratio of the slurry was 0.2 g/mL increased compared with those before CO_2 sequestration. When the S/L ratio increased to 0.4 g/mL, the development of compressive strength of CAC was little affected as the differences were within 4%. However, clear reductions (i.e. around 13.5%) on the compressive strength of CAC were observed when the S/L ratio increased to 0.6 g/mL.

Owing to the addition of $CaCO_3$, three kinds of ITZs existed in CAC after CO_2 sequestration. Therefore, further studies should be conducted to explore the microstructures (e.g., nano-mechanical properties, porosity, etc.) of these ITZs and their impacts on the durability (e.g., carbonation resistance, chloride ions penetration, etc.) of CAC.

Acknowledgements
The authors would like to thank Mr. Yunhong Luo for his help in conducting the experiments.

Authors' contributions
Investigation, methodology, data curation and formal analysis: Renjie Mi and Yifei Wang; Conceptualization: Renjie Mi and Tao Yu; Writing-original draft: Renjie Mi and Yifei Wang; Writing-review & editing: Renjie Mi, Tao Yu and Wengui Li; Supervision and resources: Tao Yu. All authors have read and agreed to the published version of the manuscript.

Funding
The authors are grateful for the financial support received from the Hong Kong Research Grants Council (Project No: T22-502/18-R), and The Hong Kong Polytechnic University (Project ID: P0039974 and 1-W18N).

Availability of data and materials
The datasets generated during and/or analysed during the current study are available from the corresponding author on reasonable request.

Declarations

Ethics approval and consent to participate
This article does not contain any studies with human participants or animals performed by any of the authors. This study was done according to ethical standards.

Consent for publication
Not applicable.

Competing interests
Tao Yu is one of the Editorial Board Members for Low-carbon Materials and Green Construction and was not involved in the editorial review, or the decision to publish, this article. All authors declare that there are no other competing interests.

Author details
[1]Department of Civil and Environmental Engineering, The Hong Kong Polytechnic University, Hong Kong, China. [2]School of Civil and Environmental Engineering, University of Technology Sydney, Sydney, NSW 2007, Australia.

Received: 14 May 2023 Revised: 1 July 2023 Accepted: 4 July 2023
Published online: 17 August 2023

References

1. Metz, B., Davidson, O., Coninck, H. d., Loos, M., & Meyer, L. (2005). *IPCC special report on carbon dioxide capture and storage*. United Kingdom and New York, NY, USA.
2. Nie, S., Zhou, J., Yang, F., Lan, M. Z., Li, J. M., Zhang, Z. Q., Chen, Z. F., Xu, M. F., Li, H., & Sanjayan, J. G. (2022). Analysis of theoretical carbon dioxide emissions from cement production: methodology and application. *Journal of Cleaner Production, 334*, 130270.
3. Liu, Y., Zhuge, Y., Chow, C. W. K., Keegan, A., Li, D. D, Pham, P. N., Huang, J. Y, & Siddique, R. (2020). Properties and microstructure of concrete blocks incorporating drinking water treatment sludge exposed to early-age carbonation curing. *Journal of Cleaner Production, 261*, 121257.
4. Mi, R. J., & Pan, G. H. (2022). Inhomogeneities of carbonation depth distributions in recycled aggregate concretes: a visualisation and quantification study. *Construction and Building Materials, 330*, 127300.
5. Dixit, A., Du, H. J., & Pang, S. D. (2021). Carbon capture in ultra-high performance concrete using pressurized CO2 curing. *Construction and Building Materials, 288*, 123076.
6. Mi, R. J., Pan, G. H., & Kuang, T. (2021). Reducing carbonation zone and steel corrosion zone widths of recycled aggregate concrete through optimizing its mixing process. *Journal of Materials in Civil Engineering, 33*(5), 04021061.
7. Mi, R. J., Yu, T., & Poon, C. S. (2023). Feasibility of utilising porous aggregates for carbon sequestration in concrete. *Environmental Research, 228*, 115924.
8. Da, B., Yu, H. F., Ma, H. Y., Tan, Y. S., Mi, R. J., & Dou, X. M. (2016). Experimental investigation of whole stress-strain curves of coral concrete. *Construction and Building Materials, 122*, 81–89.
9. Zhou, W., Feng, P., & Yang, J. Q. (2020). Advances in coral aggregate concrete and its combination with FRP: A state-of-the-art review. *Advances in Structural Engineering, 24*(6), 1161–1181.
10. Wu, W. J., Wang, R., Zhu, C. Q., & Meng, Q. S. (2018). The effect of fly ash and silica fume on mechanical properties and durability of coral aggregate concrete. *Construction and Building Materials, 185*, 69–78.
11. Wang, F., Sun, Y. Z., Xue, X. Y., Wang, N., Zhou, J. H., & Hua, J. M. (2023). Mechanical properties of modified coral aggregate seawater sea-sand concrete: Experimental study and constitutive model. *Case Study in Construction Materials, 18*, e02095.
12. Chu, Y. J., Wang, A. G., Zhu, Y. C., Wang, H., Liu, K. W., Ma, R., Guo, L. P., & Sun, D. S. (2021). Enhancing the performance of basic magnesium sulfate cement-based coral aggregate concrete through gradient composite design technology. *Composites Part B Engineering, 227*, 109382.
13. Liu, J. M., Ju, B. Y., Xie, W., Zhou, T., Xiao, H. Y., Dong, S. L., & Yang, W. S. (2021). Evaluation of the effects of surface treatment methods on the properties of coral aggregate and concrete. *Materials, 14*(22), 6784.
14. Lee, S. J., Jeong, S. H., Kim, D. U., & Won, J. P. (2020). Effects of graphene oxide on pore structure and mechanical properties of cementitious composites. *Composite Structures, 234*, 111709.
15. Chen, R. M., Mo, K. H., & Ling, T. C. (2022). Offsetting strength loss in concrete via ITZ enhancement: From the perspective of utilizing new alternative aggregate. *Cement and Concrete Composites, 127*, 104385.
16. Chung, S. Y., Kim, J. S., Kamm, P. H., Stephan, D., Han, T. S., & Abd Elrahman, M. (2021). Pore and solid characterizations of interfacial transition zone of mortar using microcomputed tomography images. *Journal of Materials in Civil Engineering, 33*(12), 04021348.
17. China Academy of Building Research (CABR) (2020). *Technical specification for coral aggregate concrete* (T/CECS 694–2020). China Planning Press.

18. Ministry of Housing and Urban-Rural Development of the People's Republic of China (MOHURD) (2019). *Standard for test methods of concrete physical and mechanical properties* (GB/T 50081–2019). China Architecture & Building Press.
19. General Administration of Quality Supervision, Inspection and Quarantine of the P.R. China (GAQSIQ) (2010). *Lightweight aggregates and its test methods-Part 2: Test methods for lightweight aggregates* (GB/T 17431.2–2010). Standards Press of China.
20. Otsu, N. (1979). A threshold selection method from gray-level histograms. *IEEE transactions on systems, man, and cybernetics, 9*(1), 62–66.
21. Yang, L., Gao, D. Y., Zhang, Y. S., Tang, J. Y., & Li, Y. (2019). Relationship between sorptivity and capillary coefficient for water absorption of cement-based materials: Theory analysis and experiment. *Royal Society Open Science, 6*(6), 190112.
22. Yu, S. W., Sanjayan, J., & Du, H. J. (2022). Effects of cement mortar characteristics on aggregate-bed 3D concrete printing. *Additive Manufacturing, 58*, 103024.
23. Du, H. J., & Pang, S. D. (2021). Long-term influence of nanosilica on the microstructures, strength, and durability of high-volume fly ash mortar. *Journal of Materials in Civil Engineering, 33*(8), 04021185.
24. Li, Y. G., Zhang, H. M., Liu, X. Y., Liu, G. X., Hu, D. W., & Meng, X. Z. (2019). Time-varying compressive strength model of aeolian sand concrete considering the harmful pore ratio variation and heterogeneous nucleation effect. *Advances in Civil Engineering*, *2019*(3), 1–15.

Publisher's Note